

# A 3-dimensional particle device simulator; HyDeLEOSMC and its application to a FinFET

Y. Ohkura, C. Suzuki, T. Enda, H. Takashino, H. Ishikawa, T. Kojima and T. Wada

Semiconductor Leading Edge Technologies, Inc.

16-1 Onogawa, Tsukuba, Ibaraki, 305-8569 JAPAN

Email: ohkura@selete.co.jp

**Abstract - A 2 and 3 dimensional ensemble Monte Carlo device simulator is developed and applied to FinFET analysis by using 'realistic' number of electrons within the channel of actual device. The result of transient fluctuation of electron numbers, currents, and distributions of potential and electron are shown.**

## I. INTRODUCTION

With the shrink of device size, the needs of the simulation for devices with multi-dimensional complicated structure are increasing. In Selete, a TCAD system, ENEXSS [1], including 3 dimensional process and device simulators has been developed for next generation devices. Also, the non-equilibrium transport and statistical dispersion is increasing to be important. Thus we developed 3 dimensional ensemble Monte Carlo device simulator.

The FinFET is considered to be one of the promising candidates for post-planar devices because the double (or tri-) gate structure suppresses the short channel effect and thus yields high drive current with low leakage [2]. And it has been investigated by using drift-diffusion device simulation [3].

The volume of channel region of FinFETs is generally very small, thus number of electrons in channel region is sometimes less than 100, and the particle simulation with 'realistic' electron number is not so heavy burden on present computer resources, so FinFET is a good example for the three dimensional Monte Carlo simulation with 'realistic' electron numbers.

In this paper, an outline of three dimensional Monte Carlo device simulator and its application to a self-aligned double-gate MOSFET structure (FinFET) are presented, with 'realistic' electron numbers. Transient fluctuation of electron numbers, currents, and distribution of potential and electron are demonstrated.

## II. SIMULATION MODEL

In our simulator, the motions of particles with both full-band structure and nonparabolic band structure including the quantization are treated with standard scattering mechanisms [4][5] such as those of acoustic and optical phonons, ionized impurities, plasmons, carrier-carrier and surface roughness. A coupled Monte Carlo-drift diffusion method [6] is employed in which Boltzmann transport equations for particles inside Monte Carlo 'window' region and current continuity equations outside 'window' region and Poisson equations are coupled self-consistently in arbitrary 2 or 3 dimensional device structure [1]. Gate injection and tunneling model [7] using the transfer matrix method are also included.

## III. SIMULATION EXAMPLES AND RESULTS

Here, a FinFET is calculated as an example of Monte Carlo simulation in 3D structure. The 1/2 structure of n-channel FinFET with 40 nm gate length of about 14 thousand nodes is shown in Fig. 1.

The 3D process steps, using HySyProS in ENEXSS [1], are summarized as follows. Boron-doped silicon layer is formed on the buried oxide, and then etched to form fin structure. Next, an isolator is deposited, and the poly-silicon phosphorus-doped source and drain are formed. Then, gate spacer  $\text{Si}_3\text{N}_4$  is then formed, and  $\text{SiO}_2$  gate oxide is deposited. Finally the gate stack is formed.

A cross section at the center of the channel is shown in Fig. 2, in which octree grids are also shown. The fin width is 20 nm, (symmetrical half side of the fin is simulated, from 0 to 0.01 micron in the y axis of the figure), and fin height is 50 nm (from 0.2 to 0.25 micron in the z axis).

The fin is surrounded by oxide films. The oxide thicknesses are 22.5 nm at front, 100 nm at back, and 2.5 nm at both sides. Thus the quantum confinement in the y-direction should be considered. So, we solved 1D Schroedinger equations by 'finer' grids (we used 64 grids) and 3D Poisson equation self-consistently [5].

Fig. 3 shows potential distribution in the center of the channel. The wider equi-potential curve interval at fin top than fin side shows the effect.

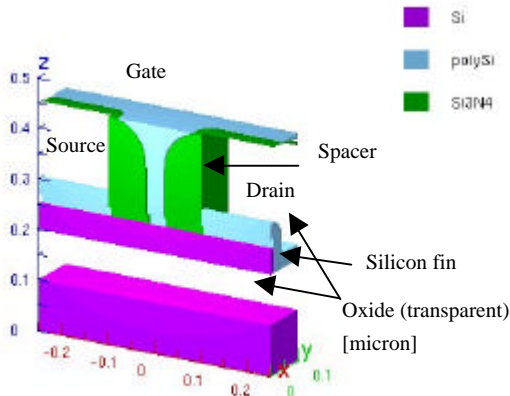


Fig. 1 Schematics of a FinFET with transparent oxide layer used in the calculation.

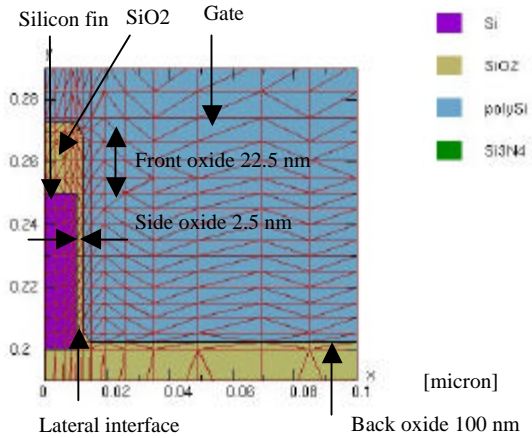


Fig. 2 A cross section at the center of the channel of the FinFET structure with octree mesh.

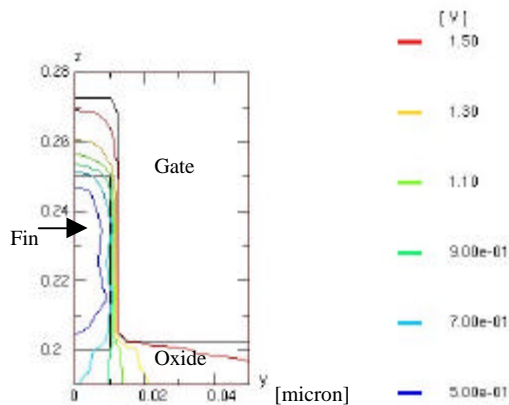


Fig. 3 Potential distribution at the center of the channel with  $V_{gs} = V_{ds} = 1.0$  V and  $V_{sub} = 0.0$ . The potential gradient at  $z = 0.25$  micron is weak compared with that at  $y = 0.01$  micron.

The  $I_d$ - $V_{gs}$  characteristics of the calculated FinFET at  $V_{ds} = 0.05$  and  $1.0$  V is shown in Fig. 4. As Monte Carlo calculation is somewhat noisy in the sub-threshold region, results of a drift diffusion model are shown here. Good sub-threshold characteristics (sub-threshold swings are about 85 mV per decade) are obtained.

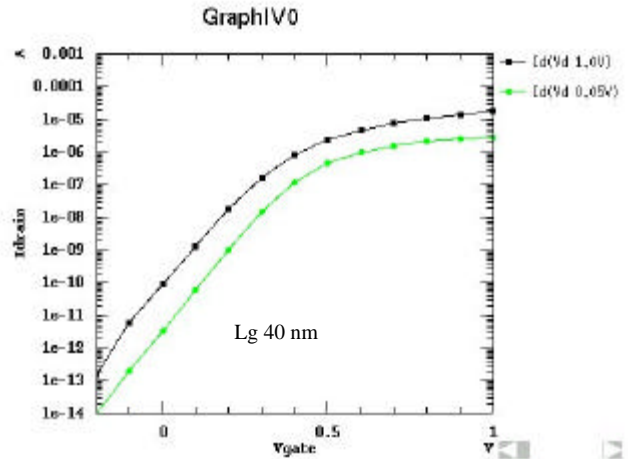


Fig. 4  $I_d$ - $V_{gs}$  characteristics of FinFET at  $V_{ds} = 0.05$  and  $1.0$  V by drift diffusion model.

A snapshot of particle distribution in the FinFET at  $V_{ds} = V_{gs} = 1.0$  V is shown in Fig. 5. Each 'globe' in Fig. 5 corresponds to a particle, whose shading denotes its kinetic energy value. The borders of Monte Carlo 'window' region are set 10 nm outside of the gate edge, so particles move in the region of 50 nm in  $x$ -direction ( $L_g 40$  nm + 10 nm), 10 nm in  $y$ -direction and 50 nm in  $z$ -direction, i.e. the volume of  $2.5 \cdot 10^{-17}$   $\text{cm}^3$  with 605 nodes. Due to the small device size, the typical number of actual electrons in the channel region is less than 100. So in this simulation, the number of particles assigned is the same as the actual number of electrons.

The number of impurities are several hundreds in the channel region, so if we include the random dopant fluctuation, some extents of fluctuations of the drain current and threshold voltage will be expected. But in this calculation we focus on the time dependent fluctuation of the particles, so the continuous impurity concentrations are employed.

In this study, scattering models for acoustic and optical phonons, and surface roughness are included for quasi-2D particles and those for acoustic and optical phonons, and classical surface scattering [8] are included for 3D particles. To include plasmon scatterings, Poisson equations are solved at every 0.5 fs. The impurity and carrier-carrier scattering are ignored to save the simulation time as they are expected to cause only a little effect on the calculation of drain current in this configuration. Approximately

2.3 hour by Compaq ES40 833MHz is required per 1 ps simulation.

Quasi-2D particles move in both x- and z-direction along the ‘lateral interface’. Their positions of y-direction depicted in Fig. 5 are at the expectation values of subbands. In this example, back and front silicon-oxide interfaces are located at  $z = 200$  nm and 250 nm respectively. In our system, a quasi-2D particle is converted to a 3D particle just before it collides at the silicon-oxide interface, and the converted 3D particle collides by specular or diffusive reflection [8], and then is converted back to a quasi-2D particle after it goes away from the interface. The energy residual in the transition from 3D particle to quasi-2D particle is minimized from the quadratic solution of non-parabolic energy dispersion strictly.

Using the particle visualization system in ENEXSS shown in Fig. 5, one can demonstrate the motion of particles due to the phonon scatterings and surface reflections and potential fluctuations.

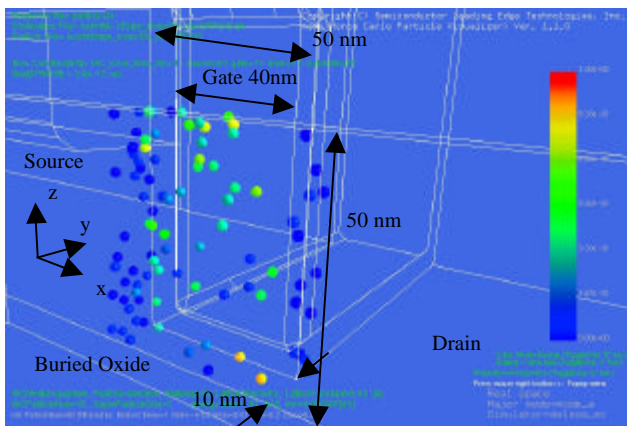


Fig. 5 A snapshot of particle distribution in the FinFET. Each globe in the center area of the figure corresponds to an electron, whose shading denotes its energy.

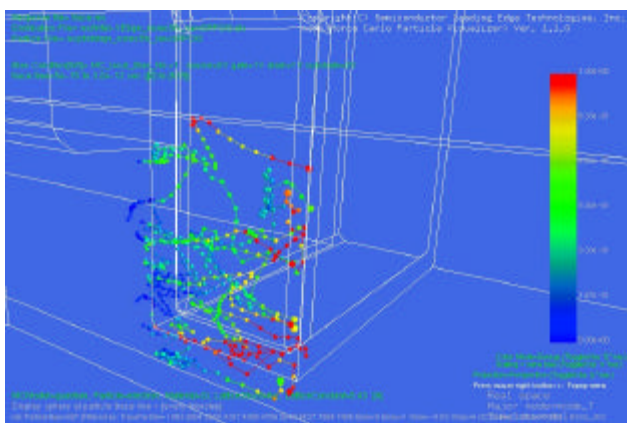


Fig. 6 Example of the traces of the particles in the FinFET.

The trace of each particle motion can be also visualized, as shown in Fig. 6. In the figure, marks are

attached in every 10 fs and the shadings of lines correspond to their kinetic energies. Particles move up and down due to scatterings, with changing their kinetic energies.

#### IV. DUSCUSSION ON FLUCTUATION

The transient number of particles in the Monte Carlo ‘window’ region is shown in Fig. 7. In the figure, the number of particle is plotted every 5 fs. In simulation particles are updated every 0.5 fs actually. The number gets stable after 0.5 ps. The average number is 94.3 and standard deviation at each time step is 4.8, which are statistically reasonable and realistic values.

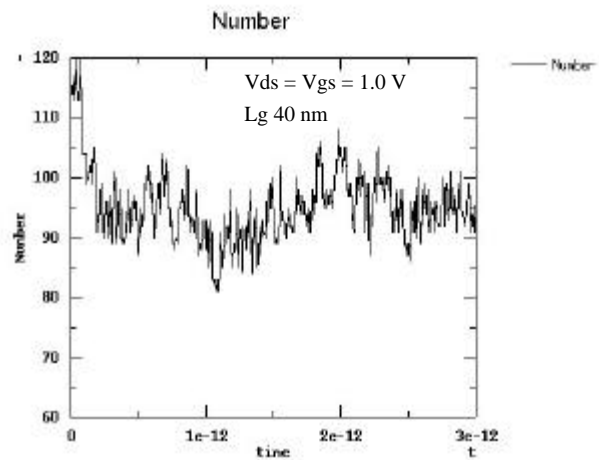


Fig. 7 The transient number of particles. From 0 ps to 3 ps.

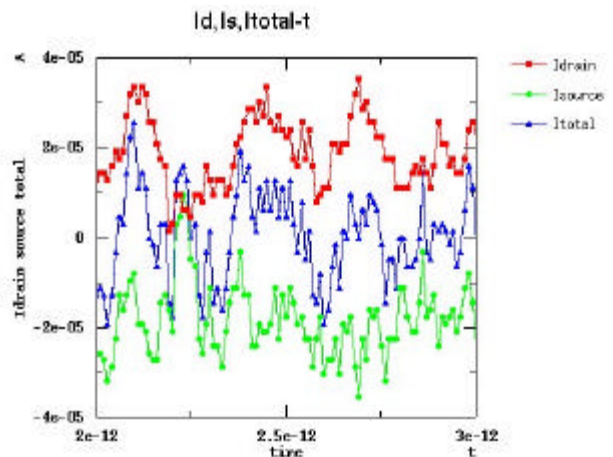


Fig. 8 The transient drain and source currents.  $V_{ds} = V_{gs} = 1.0$  V and  $V_{sub} = 0$  V. From 2 ps to 3 ps.

The transient drain and source currents from 2 ps to 3 ps are shown in Fig. 8. Average drain current is about  $1.9 \cdot 10^{-5}$  A, which means about 120 particles flows per pico second, and its standard deviation for each time step is about  $0.7 \cdot 10^{-5}$  A. These currents are defined at the source and drain contacts in the region

of drift diffusion model, and are the results of self-consistent solution of the current continuity equations at outside ‘window’ region and the Poisson equations. If the currents are defined from the particle numbers of ‘creation and annihilation’ at the borders of the Monte Carlo ‘window’ region, they should be multiple values of unit charge per update time  $[q/(dt)]$  ( $1.6 \cdot 10^{-5}$  A if numbers are counted at every 10 fs), so the currents at the contacts are smoothed compared with the currents at the borders of ‘window’ region.

The snapshot of potential distribution along the lateral interface (at  $y = 0.01$  micron in Fig. 2) is shown in Fig. 9. To solve Poisson equation, the charge of each carrier is assigned to grids based on a nearest-grid-point method in x- and z-direction considering the density of wave function of subband in y-direction. In this simulation, the potential change in Poisson updating is typically less than 10 mV. The fluctuation of the potential distribution in the figure corresponds to the electron density distribution is shown in Fig. 10. In Fig. 10, you can see several ‘needles’ that corresponds to the particle location. The height of ‘needles’ represents the number of particles assigned to each grid and the magnitude of their wave function.

## V. CONCLUSION

A 2 and 3 dimensional ensemble Monte Carlo device simulator in which 3D Poisson equation and 1D Schroedinger equation are solved self-consistently, is developed and is applied to FinFET analysis by using ‘realistic’ number of electrons within the channel of actual device. And the result of transient fluctuation of electron numbers, currents, and distributions of potential and electron are shown.

## REFERENCES

- [1] T. Wada and N. Kotani, “Design and Development of 3-Dimensional Process Simulator,” IEICE Trans. Electron., E82-C, pp. 839-847 (1999).
- [2] X. Huang, W. Lee, C. Kuo, D. Hisamoto, L. Chang, J. Kedzierski, E. Anderson, H. Takeuchi, Y. Choi, K. Asano, V. Subramanian, T. King, J. Bokor, and C. Hu, “Sub 50-nm FinFET: PMOS”, IEDM Tech. Digest, pp. 67-70 (1999).
- [3] M. Kondo, R. Katsumata, H. Aochi, T. Hamamoto, S. Ito, N.Aoki, and T. Wada, “A FinFET Design Based on Three-Dimensional Process and Device Simulations”, SISPAD 2003, pp. 179-182.
- [4] C. Jacoboni and P. Lugli, “The Monte Carlo Method for Semiconductor Device Simulation”, Springer-Verlag, Wien-New York (1989).
- [5] M. V. Fischetti and S. E. Laux, “Monte Carlo study of electron transport in silicon inversion layers”, Phys. Rev. B

48, pp. 2244-2274 (1993).

- [6] D. Y. Cheng, C. G. Hwang, and R. W. Dutton, “PISCES-MC: a multiwindow, multimethod 2-D device simulator”, IEEE Trans. Computer Aided Design, 9, pp. 1017-1026 (1988).
- [7] Y. Ohkura, C. Suzuki, H. Amakawa and K.Nishi, “Analysis of gate currents through High-K dielectrics using a Monte Carlo Device Simulator”, SISPAD 2003, pp. 67-71.
- [8] Y. Park, T. Tang and D. H. Navon, “Monte Carlo surface scattering simulation in MOSFET structures”, IEEE Trans. Electron Devices, 30, pp. 1110-1115 (1983).

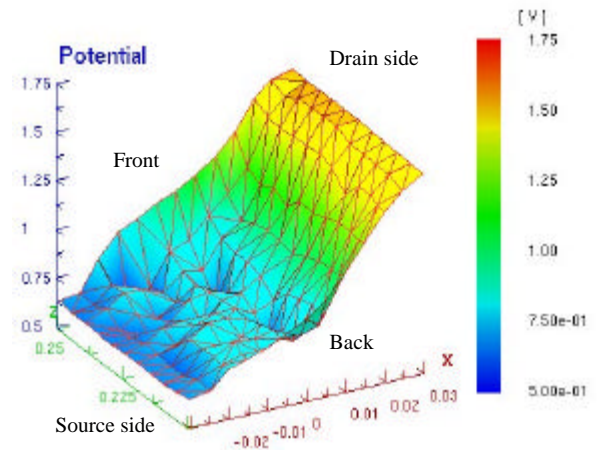


Fig. 9 Potential distribution along lateral silicon-oxide interface (at  $y = 0.01$  micron in Fig. 2).  $V_{ds} = V_{gs} = 1.0$  V with ‘realistic’ electrons.

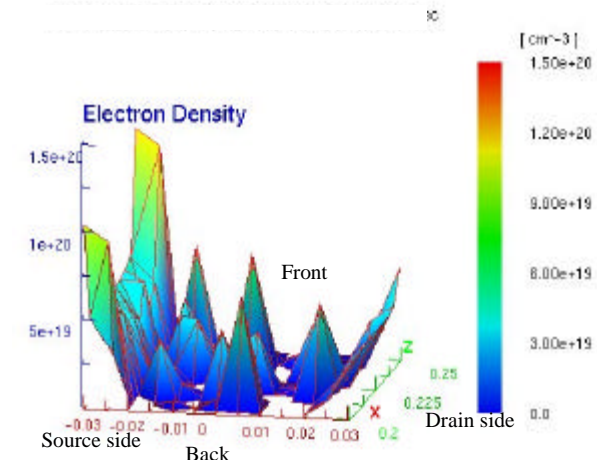


Fig. 10 Electron distribution along lateral silicon-oxide interface.  $V_{ds} = V_{gs} = 1.0$  V with ‘realistic’ electrons. Electron concentration is assigned to the grids of 2.5 nm by 2.5 nm.